# Coherent contributions of charge-dependent forces to the spreading width of the analog of $^{49}$Ca

G. K. Kim* and W. M. MacDonald
*Department of Physics and Astronomy, University of Maryland, College Park, Maryland 20742*
(Received 10 June 1985)

We report on a microscopic calculation of the spreading width $\Gamma_A^{\downarrow}$ of the isobaric analog state in $^{49}$Sc of the ground state of $^{49}$Ca. In calculating the coupling of the isobaric analog state to hallway states we included (1) first and second order Coulomb coupling, (2) a charge-dependent but charge-symmetric interaction from the mass difference between charged and neutral pions, and (3) a charge-asymmetric interaction fitted to the Coulomb displacement anomaly in $^{41}$Sc-$^{41}$Ca. The second order Coulomb terms arise from mixing with the $T=\frac{7}{2}$ component of a giant isovector monopole. The different sets of matrix elements are found to add coherently to give $\Gamma_A^{\downarrow}=5$–$7$ keV, in excellent agreement with the value of $\Gamma_A^{\downarrow}=5.3$ keV which we obtain from a strength function analysis of the high resolution data on $^{48}$Ca(p,p). The coherent charge-symmetric–charge-dependent contribution gives approximately one-half of $\Gamma_A^{\downarrow}$. The result for $\Gamma_A^{\downarrow}$ also includes a charge-asymmetric reduction of about 1 keV, but this is too small to confirm its presence in view of the uncertainty in the value of $\Gamma_A^{\downarrow}$.

## I. INTRODUCTION

The fragmentation of a nuclear isospin state which is seen in high resolution data on an isobaric analog resonance (IAR) is the most visible evidence for the breaking of nuclear isospin symmetry by charge-dependent interactions. The microresonances seen, for example, in (p,p) scattering on a nucleus with $T_3=\frac{1}{2}(N-Z)$ results from the coupling of the isobaric analog state (IAS) with isospin $T_>=T_3+1$ to more numerous states with isospin $T_<=T_3$. In low resolution experiments the isospin mixing is seen as an additional "spreading width," $\Gamma_A^{\downarrow}=\Gamma_A-\sum_c\Gamma_{Ac}$. The Coulomb force is usually held to be responsible for this mixing, but its long-range character reduces its direct coupling matrix elements so much that a second-order coupling dominates. Assuming that the dominant mechanism involves Coulomb coupling the IAS to the giant isovector monopole (IVM) excitation and an antianalog state, both states with $T_<$ which are coupled to "fine structure" (FS) states near the IAS by the charge-independent component of the two-nucleon force, Mekjian[1] was able to account for the systematic behavior of $\Gamma_A^{\downarrow}$ in various nuclei.

It is not obvious, however, that the contribution to $\Gamma_A^{\downarrow}$ of the known charge-dependent components of the short-range two-nucleon interaction can be neglected relative to the second-order Coulomb interaction. In fact, since a short-range interaction is effective in coupling the IAS directly to nearby $T_<$ states, we should expect its contribution to the spreading width to be enhanced relative to that of the Coulomb interaction. The spreading width might therefore be expected to be a more sensitive measure of the charge-dependent components of the short-range interaction between nucleons than level shifts between corresponding states in an isobaric multiplet. In this paper we investigate the contribution to $\Gamma_A^{\downarrow}$ of, first, the well-established charge-symmetric–charge-dependent (CSCD) interaction arising in large part from the difference in mass between charged and neutral pions. To this we add a charge-asymmetric–charge-dependent (CACD) interaction whose magnitude we fix to account for the Nolen-Schiffer anomaly in $^{41}$Sc-$^{41}$Sc.[2] There is theoretical justification for a CACD interaction which will fit the scattering data, although Shlomo[3] has argued that the same interaction cannot fit Coulomb anomalies in both light and heavy mirror nuclei. For this reason we consider it important to investigate the limitations on the magnitude of the CACD interaction which the measured spreading widths might provide.

Inclusion of the CSCD and the CACD interactions in the calculation of a spreading width requires inclusion also of the Coulomb matrix elements which couple the IAS directly to nearby $T_<$ states. This necessarily leads to an extensive microscopic calculation in which these interactions contribute coherently to the spreading width. The possible importance of constructive and destructive interference between various contributions to the coupling between an IAS and a given FS state of $T_<$ also forces abandonment of the schematic treatment of the second-order spreading used by Mekjian. In this paper we present a way of including the second-order Coulomb coupling through the IVM as a coherent contribution to the spreading width. We shall see that this is very important because the short-range charge-dependent interactions contribute coherently to the spreading width.

The large scale of a microscopic calculation of a spreading width has limited us to consideration of the $J^{\pi}=\frac{3}{2}^-$ IAR observed in (p,p) and (p,n) reactions on $^{48}$Ca by Wilhjelm *et al.*[4] This resonance corresponds to a $T=\frac{9}{2}$ state in $^{49}$Sc which is the IAS of the ground state of $^{49}$Ca. This high resolution experiment showed the existence of eight fragments of this IAS and determined the

 

energy and width of each fragment. As we shall show in Sec. II, a strength function analysis of the distribution of widths allows us to determine $\Gamma_A^{\downarrow}=5.3\pm0.5$ keV. This IAS is particularly suitable for a microscopic calculation of the spreading width because $^{48}$Ca has been shown to be a particularly good approximation to a closed shell nucleus.[5] Moreover, an unrestricted Hartree-Fock calculation[6] of the isospin impurity of this nucleus gives a very small result, $\alpha^2=0.0016$. This result allows us to use perturbation theory to calculate the isospin mixing produced by the Coulomb force and the CSCD and CACD interactions in this nucleus. Even so, we find it necessary to develop a variety of new techniques in order to carry out the calculation of the spreading width of this IAS.

In Sec. II we present the theory needed to relate the experimentally determined $R$-matrix parameters to corresponding quantities in a unified shell model reaction theory, discuss the strength function for an IAS, and give a strength function analysis of the isobaric analog of the ground state of $^{49}$Ca to determine its spreading width $\Gamma_A^{\downarrow}$. Section III develops equations for calculating the contribution to the spreading width of the isovector monopole term in the Coulomb field and specifies the short-range CSCD and CACD interactions used in this calculation. Section IV presents various aspects of the microscopic calculation, including (1) a comparison between the observed level spacing and that obtainable from 2p-1h, 3p-2h, 4p-3h, etc., excitations; (2) a reduction of the equation for the spreading width to one containing only matrix elements to "hallway states"; and (3) a brief discussion of the techniques developed to construct hallway states of good isospin and to evaluate the matrix elements connecting them to the IAS. Section V presents the results of the calculations. Section VI summarizes our conclusions.

## II. THEORY

### A. Resonance parameters of the $K$ matrix

The IAR is an intermediate resonance which can be seen in high resolution experiments as a number of microresonances having the same spin and parity with widths increasing toward the center of the pattern.[7] An $R$-matrix analysis of the high resolution data gives the resonance parameters $\{E_\lambda,\gamma_{\lambda c}^2\}$ for each of the microresonances. Since we want to carry out a microscopic shell model calculation, based on the antisymmetrized products of single-particle states, we use the $K$-matrix formulation of the shell model reaction theory.[8] After a brief summary of this theory we shall then relate its resonance parameters to those from the $R$-matrix analysis.

The $S$ matrix is given by

$$S_{cc'}=\exp[i(\delta_c+\delta_{c'})][(1+iK)(1-iK)]_{cc'} , \tag{2.1}$$

where $\delta_c$ is the phase shift for a one-body potential $U$. The $K$ matrix includes both a direct and a resonant term,

$$K_{cc'}=K_{cc'}^D+K_{cc'}^R , \tag{2.2}$$

with

$$K_{cc'}^D=\pi\langle cE \mid V_e \mid c'E\rangle , \tag{2.3}$$

$$K_{cc'}^R=\tfrac{1}{2}\sum_\lambda \frac{\Gamma_{\lambda c}^{1/2}\Gamma_{\lambda c'}^{1/2}}{(E-E_\lambda)} . \tag{2.4}$$

The term $K_{cc'}^D$ is a direct transition matrix element between continuum channels for the $A$-nucleon system, each of which is the antisymmetrized product of bound states $\Phi_\beta$ for the target or residual nucleus and a continuum single-particle state in the potential $U$.

$$\mid cE\rangle=\mathcal{A}\Phi_\beta(1,\ldots,A-1)u_{jl\epsilon}(A) . \tag{2.5}$$

Here $c\equiv(\beta jl\epsilon)$ denotes the channel quantum numbers, which include the single-particle angular momentum quantum number and its energy $\epsilon$.

The individual terms of $K_{cc'}^R$ describe compound nuclear resonances corresponding to eigenstates $\Psi_\lambda$ which diagonalize an effective Hamiltonian $H_S=H_0+QV_eQ$ on the set of discrete states $\mid\alpha\rangle$ containing only bound single-particle orbitals.

$$\langle 1,\ldots,A \mid \alpha\rangle=\mathcal{A}\prod_{i=1}^{A}\langle i \mid \alpha_i\rangle . \tag{2.6}$$

The effective interaction $V_e$ which appears in these equations includes both the lowest order direct interactions with the target through the residual interaction $V=H-H_0$ and multistep reaction processes. If $P$ projects onto the continuum states and $Q=1-P$ projects onto the discrete states, the effective interaction is given by

$$V_e=V+VP(E-H_0-V)^{-1}PV . \tag{2.7}$$

The compound states satisfying

$$\langle\Psi_\lambda \mid H_S \mid \Psi_\mu\rangle=\delta_{\lambda\mu}E_\lambda \tag{2.8}$$

therefore include both level shifts and configuration mixing arising from the coupling to open channels. These effects come from the second term in the equation for $V_e$. The decay amplitudes for the compound states are given by

$$\Gamma_{\lambda c}(E)^{1/2}=(2\pi)^{1/2}\langle\Psi_\lambda \mid V_e \mid cE\rangle . \tag{2.9}$$

We now relate these $K$-matrix quantities to the corresponding $R$-matrix parameters. For simplicity we consider the case of only one open channel; the same discussion applies to more than one open channel. In a narrow energy interval the $R$-matrix equation for the $S$ matrix can be written

$$S_{cc}=\exp(2i\varphi_c)\frac{1-iP_c\sum_\lambda\gamma_{\lambda c}^2/(E-E_\lambda)}{1+iP_c\sum_\lambda\gamma_{\lambda c}^2/(E-E_\lambda)} . \tag{2.10}$$

To compare with the corresponding $K$-matrix equation we must choose the single-particle potential $U$ so that the phase shifts $\delta_c$ give the nonresonant elastic scattering at low energies. This choice makes $K_{cc}^D=0$, and in the single channel case reduces Eq. (2.1) to

$$S_{cc}=\exp(2i\delta_c)\frac{\frac{1}{2}i\sum_\lambda\Gamma_{\lambda c}/(E-E_\lambda)}{\frac{1}{2}i\sum_\lambda\Gamma_{\lambda c}/(E-E_\lambda)} . \tag{2.11}$$

Although the hard-sphere phase shift $\varphi_t$ and the potential phase shift $\delta_c$ differ greatly in their energy dependence far from threshold, both must fit the nonresonant background at low energies. In $R$-matrix fits to cross sections the channel radius can be adjusted to fit the nonresonant background, giving $\varphi_t \simeq \delta_c$ across the fine structure pattern of an IAR.

For the narrow resonances observed in the IAR it is clear that the resonance energies $E_\lambda$ and widths on resonance must be equal,

$$\Gamma_{\lambda c}(E_\lambda)=2P_c(E_\lambda)\gamma_{\lambda c}^2 .$$

We note that the $K$-matrix width given by Eq. (2.9) has an energy dependence due simply to the penetrability of the emitted particle. Calculations by one of us (W.M.M.) show that this energy dependence is accurately given by the $R$-matrix penetrabilities $P_c$. We can therefore use the $R$-matrix definition of the reduced widths,

$$\Gamma_{\lambda c}(E)=2P_c(E)\gamma_{\lambda c}^2 . \tag{2.12}$$

This equation enables us to use $R$-matrix reduced widths to determine a spreading width $\Gamma_A^\downarrow$ for the IAS. We shall then go on to calculate $\Gamma_A^\downarrow$ using shell model wave functions and the known (and suggested) charge dependent interactions.

### B. Strength function for the $K$ matrix

The reduced widths observed in an IAR define very roughly an envelope which peaks near the unperturbed IAS. The reduced width of each microresonance is proportional to the fraction of the IAS present in the corresponding $\Psi_\lambda$ and therefore to the isospin-violating matrix element between the IAS and a FS state with $T_<$. Statistical fluctuations in this matrix element are largely responsible for the deviations from a Lorentzian envelope. To obtain information about the magnitude of the charge-dependent interactions we use a strength function (SF) which is the Lorentz-weighted average of the reduced widths.[9–11]

$$S(E;I)\equiv(I/\pi)\sum_\lambda \frac{\gamma_{\lambda c}^2}{(E-E_\lambda)^2+I^2} . \tag{2.13}$$

The averaging half-width $I$ is arbitrary and can be chosen to give a smooth function of energy.

A remarkable property of this strength function is that near an IAR it has a characteristic energy dependence

$$S(E;I)=s_c+\frac{\gamma_{Ac}^2}{\pi\cos^2\varphi} \times\frac{(\Gamma_A^\downarrow/2+I)\cos2\varphi-(E-E_A-\Delta_A)\sin2\varphi}{(E-E_A-\Delta_A)^2+(\Gamma_A^\downarrow/2+I)^2} . \tag{2.14}$$

The quantities $E_A$ and $\gamma_{Ac}^2$ are the energy and reduced width of the unperturbed IAS. The remaining four parameters $s_c$, $\Gamma_A^\downarrow$, $\Delta_A$, and $\varphi_A$ are Lorentz-weighted averages of *microscopic* quantities. Let $\epsilon_f$ denote the energy of a FS state of "intrinsic" partial width $\gamma_{ic}$ which is coupled to the IAS by a matrix element $M_f$. Then defining the average distribution of any microscopic quantity $q_f$ by

$$\langle q_f/D_f\rangle\equiv\frac{I}{\pi}\sum_f\frac{q_f}{(E-\epsilon_f)^2+I^2} , \tag{2.15}$$

we can write succinct equations for the parameters in Eq. (2.14). The level spacing $D_f$ appears in this definition, but it is not actually used to calculate the quantity on the left. One might be tempted to write $\langle f_f\rangle=\langle f_f/D_f\rangle\langle D_f\rangle$, but the density of levels is not high enough to define a *local* average level density. Therefore, the quantity on the left must be understood as a symbol for the sum on the right.

$$\Gamma^\downarrow=2\pi\langle M_f^2/D_f\rangle , \tag{2.16a}$$

$$\Delta_A=\langle M_f^2(E-\epsilon_f)/D_f\rangle , \tag{2.16b}$$

$$s_c=\langle\gamma_{fc}^2/D_f\rangle , \tag{2.16c}$$

$$\tan\varphi=-\pi\langle M_f\gamma_{fc}/D_f\rangle/\gamma_{Ac} . \tag{2.16d}$$

It is important to realize that the characteristic pattern of reduced widths observed in the IAR, large near $E_A$ and decreasing rapidly away from it, does not come from a resonance in the coupling matrix elements but from the energy denominators $(E_A-\epsilon_f)^2$ of perturbation theory. The coupling matrix elements undoubtedly extend to states many MeV above, and even below, the IAS, even though the spreading widths range from a few keV to a few tens of keV at most. The matrix elements can be expected to have random phases with magnitudes that exhibit statistical fluctuations, but for values of $I$ somewhat larger than the average level spacing the parameters above are nearly constant and independent of the precise value of $I$. A model study[12] has shown that an average interval $I\sim\Gamma^\downarrow$ gives a strength function from which the spreading width can be determined with an uncertainty of about 10%.

### C. SF analysis of the isobaric analog of the ground state of $^{49}$Sc

High resolution excitation functions from $^{48}$Ca(p,p) and $^{48}$Ca(p,n) between $E_p=1.93$ and 2.01 MeV reveal the existence of eight $J^\pi=\frac{3}{2}^-$ resonances whose energies and reduced widths are given in Table I and illustrated in Fig.

TABLE I. $R$-matrix resonance parameters for $J^\pi=\frac{3}{2}^-$ in $^{49}$Sc.

| $E_\lambda$ (c.m.) (keV) | $\gamma_{\lambda p}^2$ (c.m.) (keV) |
|---|---|
| 1908±2 | 0.844 |
| 1919±2 | 2.716 |
| 1922±2 | 0.134 |
| 1924±2 | 8.026 |
| 1934±2 | 33.659 |
| 1941±2 | 1.014 |
| 1942±2 | 1.264 |
| 1950±2 | 0.492 |

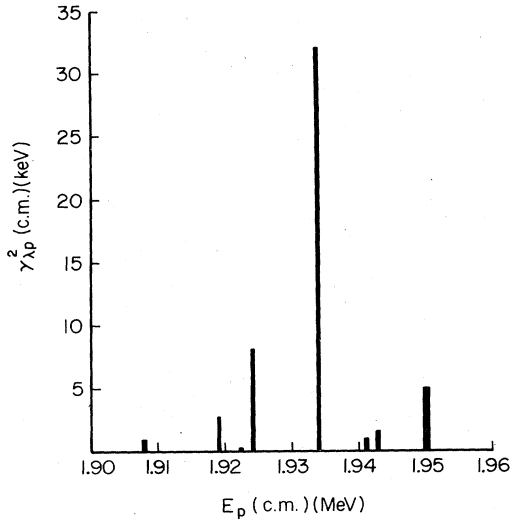


FIG. 1. Reduced widths for proton emission from states in $^{49}$Sc belonging to the IAR corresponding to the ground state of $^{49}$Ca. The abscissa is the excitation energy of $^{49}$Sc.

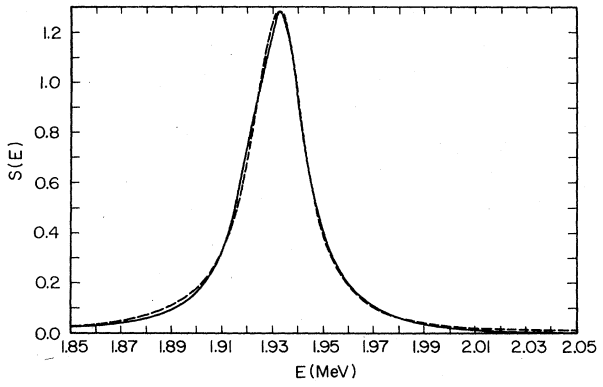


FIG. 2. Strength function of the $^{49}$Ca analog for $I=10$ keV. The solid curve is calculated from Eq. (2.13) using experimental resonance parameters from Table I. The dashed curve is the fitted doorway strength function given by Eq. (2.14) for the parameters in Table II.

1. The average level spacing is $\langle D_f \rangle \sim 6$ keV. Figure 1 shows the SF for $I=10$ keV. This SF has a clearly defined width at half-maximum of about 26 keV. The intrinsic widths of the $T_<$ states are so small, seen in the reduced widths well away from the central peak, that one can take $s_c$ to be zero in estimating the width of the SF. From Eq. (2.14) one sees that $\Gamma^{\downarrow} \simeq 26$ keV $-2I=6$ keV. A more reliable determination is done by using a nonlinear least-squares procedure to determine the parameters in Eq. (2.14) by fitting to the SF calculated from Eq. (2.13) with the $(E_\lambda, \gamma^2_{\lambda c})$ given in Table I. The quality of the fit to the strength function is shown in Fig. 2, where the dashed line represents Eq. (2.14). The parameters obtained from this analysis are given in Table II.

## III. CHARGE-DEPENDENT INTERACTIONS AND THE GIANT ISOVECTOR MONOPOLE

The charge-dependent interactions in the nuclear Hamiltonian include the Coulomb interaction together with isovector and isotensor terms in the short-range two-nucleon interaction. These latter are small compared to the isoscalar terms in the two-nucleon interaction, and this suggests a perturbation calculation based on nuclear wave functions of pure isospin. The Coulomb distortion of the continuum proton states cannot be treated perturbatively, however, so we are obliged to include the asymptotic part of the average Coulomb interaction in the independent-particle Hamiltonian $H_0$. The smallness of the spreading width of an IAS requires that care be given to setting out the framework of the calculation, as we do in this section.

### A. The IAS and the choice of $H_0$

The IAS is defined by the equation

$$|A\rangle \equiv T_- |P\rangle (2T_<)^{-1/2} , \tag{3.1}$$

where $|P\rangle$ is the parent, in our case, the ground state of $^{49}$Ca. As noted in Sec. I, the ground state of $^{48}$Ca is an extremely good approximation to a doubly closed shell nucleus. We therefore approximate the ground state of $^{49}$Ca as a $2p_{3/2}$ neutron coupled to this state.

The independent particle Hamiltonian $H_0$ which provides the neutron and proton radial wave functions must be chosen so that the quasibound configurations $|\alpha\rangle$ of Eq. (2.6) have negligible isospin impurity. At the same time the proton continuum wave functions must include the average Coulomb field outside the nucleus. The average Coulomb field is approximated by that of a uniformly charged sphere.

$$U_C = (Ze^2/2R^3) \sum_{i=1}^{i=A} (R^2 - r_i^2/3)(\tfrac{1}{2} - t_{3i}) \quad r_i \le R ,$$
$$= \sum_{i=1}^{i=A} (Ze^2/r_i)(\tfrac{1}{2} - t_{3i}) \quad r_i \ge R . \tag{3.2}$$

Inclusion in $H_0$ of the external Coulomb field ($r > R$) gives bound state neutron and proton radial wave func-

TABLE II. IAS parameters for the $J^\pi = \frac{3}{2}^-$ in $^{49}$Sc.

| $I$ (keV) | $E_A$ (keV) | $\gamma^2_A$ (keV) | $\Gamma^{\downarrow}_A$ (keV) | $s_0$ | $\varphi$ (rad) |
|---|---|---|---|---|---|
| 10 | 1932.4±0.3 | 51.4±0.5 | 5.3±0.1 | 0.001±0.001 | 0.017 |

tions which are identical over the nuclear interior, except for a normalization factor. The compound nuclear wave functions which diagonalize the charge-independent part of $H_S$, the effective shell model Hamiltonian, will then have very pure isospin. The remaining part of the average Coulomb field, that interior to the nucleus, is responsible for an isovector monopole deformation of the IAS which will be discussed in the next section.

The matrix elements between the IAS in $^{49}$Sc and the FS states can be written in the form

$$M_{Af}=\langle f\,|\,[V_e,T_-]\,|\,P\rangle(2T_<)^{-1/2}\,. \tag{3.3}$$

This equation follows from Eq. (3.1) and from $T_+\,|\,f\rangle=0$. The matrix element is one between the ground state of $^{49}$Ca and FS states in $^{49}$Sc of $T_<=\frac{7}{2}$. We stress that the FS states used in a microscopic calculation of the spreading width must be eigenstates of isospin. As we shall see, these states are quite complicated because they contain sums over particle-hole states of varying degrees of excitation.

Equation (3.3) makes explicit the fact that only the charge-dependent components of the effective interaction given by Eq. (2.7) contribute to the spreading matrix elements. In the succeeding subsections we shall identify these components and show how they contribute.

### B. Contribution of the average Coulomb field to $\Gamma^{\downarrow}$

As noted in the Introduction, the essential difficulty in calculating the contribution of the average interior Coulomb field to the spreading width is that it first occurs in second order perturbation theory. Nevertheless, it is large because the contribution is the product of a matrix element of the monopole Coulomb interaction and of the *charge independent* component of the effective two-nucleon interaction. This second order Coulomb coupling between the IAS and the FS states is illustrated in Fig. 3.

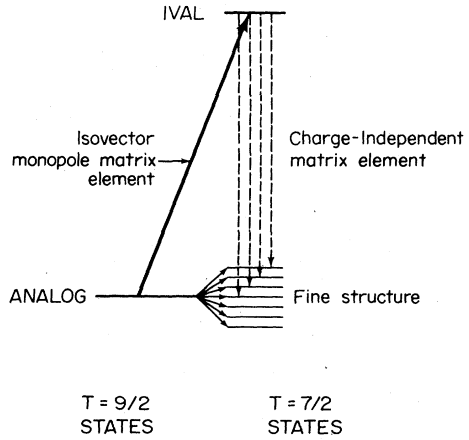


FIG. 3. Illustration of the first and second order Coulomb coupling between the IAS and FS states. The $T=\frac{9}{2}$ IAS is coupled by the Coulomb isovector monopole to the $T=\frac{7}{2}$ component of the corresponding IVM, which is coupled downward to the $T=\frac{7}{2}$ states by the charge-independent two-nucleon interaction.

We briefly summarize the doorway formalism used by Mekjian[1] to calculate this contribution and explain the necessity for a microscopic calculation.

#### *1. Doorway model*

Since the exterior part of this interaction has been included in $H_0$, we are now considering only the part of Eq. (3.2) for $r\leq R$. This monopole interaction couples the IAS to p-h excitations produced by exciting protons from $(njl)$ states to states with quantum numbers $(n+1lj)$. The first calculations of isospin mixing[13] used energy denominators from first-order perturbation theory, viz., the single-particle spacing. Later hydrodynamic calculations by Bohr, Damgaard, and Mottelson[14] led to recognition that the isovector monopole interaction generates from the IAS a collective state whose energy lies considerably above that of the individual excitations. This giant isovector monopole state[15] is defined by the equation

$$|\,M\rangle=\mathscr{M}\,|\,A\rangle/\langle A\,|\,\mathscr{M}^2\,|\,A\rangle\,, \tag{3.4}$$

where we have introduced the isovector monopole operator

$$\mathscr{M}=\sum_i r_i^2 t_{3i}\,. \tag{3.5}$$

In a nucleus with a neutron excess the state defined by this equation has several isospin components, i.e., $T_>-1$, $T_>$, and $T_>+1$, where $T_>$ is the isospin of the IAS. These components are split by the charge-independent part of the nucleon-nucleon interaction into three states of pure isospin. The relevant component of the IVM for the spreading width calculation is that with isospin $T_<\equiv T_>-1$. Coupling between the IAS and this component introduces an isospin impurity into the IAS, through which it can be coupled to the FS states with isospin $T_<$ by the charge-independent two-nucleon interaction. Auerbach[16] estimated that this component of the IVM is separated from the IAS by an energy

$$\Delta E=170A^{-1/3}-110(T_<+1)A^{-1}\,. \tag{3.6}$$

This energy approximates to $3\hbar\omega$.

Auerbach has also shown that, within the restricted basis provided by the p-h states, the IVM has a 95–97% overlap with the corresponding eigenstates of the nuclear Hamiltonian. However, the $T_<$ component of the IVM is fragmented through coupling to 2p-2h states of the same isospin by the charge-independent component of the effective interaction $V_e$. The theory of the strength function given in Sec. II would predict a Lorentzian distribution of this state among eigenstates of the full Hamiltonian with a spreading width estimated to be about 10 MeV. Using this theory Mekjian[1] calculated the spreading widths of the IAS in a number of nuclei from the equation

$$\Gamma_A^{\downarrow}=\frac{M_{AM}^2\Gamma_M^{\downarrow}}{(E_A-E_M)^2+(\Gamma_M^{\downarrow}/2)^2}+\sum_c\frac{M_{Ac}^2\Gamma_c^{\downarrow}}{(E_A-E_c)^2+(\Gamma_c^{\downarrow}/2)^2}\,, \tag{3.7}$$

where $\Gamma_M^{\downarrow}$ and $\Gamma_c^{\downarrow}$ are the spreading widths of the IVM

and of the so-called "configuration states," respectively. The latter are $T_<$ states belonging to the same configuration as the IAS. The matrix elements coupling the IAS to the IVM and configuration states are denoted by $M_{AM}$ and $M_{Ac}$. The first term of this equation represents the IAS spreading as a second-order process in which the IAS is coupled by charge-dependent forces to the IVM, which itself is spread among FS states. The global fit by Mekjian to the known $\Gamma^{\downarrow}$ used 3 MeV for the spreading width of the IVM. According to Mekjian only the IVM contributes to the spreading width in $^{49}$Sc. Using the calculated $M_{AM}$ Mekjian obtained a spreading width of 3 keV. This should be compared with the experimental value of 6 keV obtained in Sec. II.

The contribution of the IVM to the spreading width of an IAS can be calculated directly by recognizing that their coupling produces an isospin mixed wave function $|A'\rangle$ for the IAS. (Since only the $T_<$ component of the IVM enters here, we henceforth use $|M\rangle$ to denote only this component.)

$$|A'\rangle = |A\rangle + \frac{|M\rangle\langle M|U_C|A\rangle}{E_A - E_M} . \tag{3.8}$$

The IVM component of the IAS can then be coupled to the FS states near the IAS by the charge-independent two-nucleon interaction. The spreading width will depend on the structure of the FS states near the IAS, their density, and their distances from the IAS.

Equation (3.7) assumes that the spreading width to FS states near the IAS is just as large as to FS states near the IVM itself. Since the IVM in $^{49}$Sc is located some 20 half-widths above the IAS, this assumption is extremely dubious. We shall therefore explicitly calculate the contribution of the IVM to the spreading width of the $J^{\pi}=\frac{3}{2}^{-}$ IAS in $^{49}$Sc.

#### 2. Microscopic theory

The particle states in the p-h configurations making up the IVM belong mostly to the continuum of $H_0$ because the monopole operator in Eq. (3.5) excites nucleons through $2\hbar\omega$. From Eq. (3.4) it can be seen, however, that the wave function for the IVM decays exponentially because the IAS wave function contains only bound particle-hole configurations. The IVM is therefore a normalizable "packet" of continuum states of $H_0$ which can be projected out of the open channel states. This process greatly reduces the coupling of the IAS to the open channels.[17] Let $P_M = |M\rangle\langle M|$ be the projection operator for the IVM. Inclusion of the IVM among the set of discrete states is accomplished by defining $Q' = Q + P_M$ and $P' = P - P_M$. The equation for the modified shell model Hamiltonian for the compound nuclear states is obtained from Eq. (2.7) simply by replacing $P$ by $P'$. The direct coupling between the IVM and the IAS through the isovector part of $U_C$ produces the isospin mixed IAS wave function of Eq. (3.8). The matrix element coupling this state to the nearby FS states with $T_<$ is

$$M_{Af}^{(2)} = \langle f|V_{CI}|A'\rangle = \frac{\langle f|V_{CI}|M\rangle\langle M|U_C|A\rangle}{(E_A - E_M)} . \tag{3.9}$$

We now show that this second order contribution can be approximated by the matrix element of an effective interaction.

#### 3. An effective interaction for second order Coulomb mixing

The FS states responsible for the spreading width of the IAS belong to low-lying configurations which do not include the p-h states $2\hbar\omega$ which are excited by the Coulomb isovector monopole. The $V_{CI}$ must couple these FS states to the particle state excited by $U_C$. In configuration space $V_{CI}$ must deexcite the same *particle* as $U_C$ excites. The above second-order matrix element can therefore be approximated by the first-order matrix element,

$$M_{Af}^{(2)} \simeq \langle f|U_{\text{eff}}|A\rangle , \tag{3.10}$$

of an effective interaction $U_{\text{eff}}$.

$$U_{\text{eff}} = \frac{Ze^2/2R^3}{E_A - E_M}\sum_{i,j} v_{CI}(i,j) r^2(i) t_3(j) . \tag{3.11}$$

For Eq. (3.10) to be exact, the Coulomb monopole operator $r^2 t_3$ in $U_{\text{eff}}$ must not couple the IAS to $T_<$ configuration states. Now if the s.p. matrix elements of this operator are the same for all the valence nucleon orbitals it can then be replaced by the operator $cT_3$, which clearly cannot couple states of different isospin. The valence nucleon orbitals in $^{49}$Sc are $1f_{7/2}$ and $2p_{3/2}$, for which the single particle matrix elements of $r^2$ are exactly equal in the harmonic oscillator shell model basis. Consequently, Eqs. (3.10) and (3.11) are very well satisfied for the IAS we are considering. In other nuclei the relative size of the error introduced is proportional to the ratio $(M_{AM})^2/\langle M_{Ac}\rangle^2$ of the squares of the matrix elements in Eq. (3.7).

To simplify further the calculation of the contribution of the Coulomb isovector monopole to the spreading width we use a delta function representation of $v_{CI}$ which has been employed in a number of nuclear studies.[18]

$$v_{CI}(1,2) = -V_0(\pi_t + p\pi_s)\delta(\mathbf{r}_i - \mathbf{r}_j) . \tag{3.12}$$

Here $\pi_t, \pi_s$ are projection operators onto the triplet and singlet spin states of two nucleons. With the Soper mixture, for which $p=0.46$, an appropriate value of $V_0$ for $^{49}$Sc is $V_0 = 650$ MeV fm$^3$.

### C. Two-body charge-dependent interactions

We now discuss the short-range two-body interactions which contribute to the spreading width of an IAS.

#### 1. Two-body Coulomb interaction

In the preceding section we considered only the contribution of the monopole term in the Coulomb interaction. Higher multipole terms contribute to the spreading width in first order. These have often been neglected. We have included direct coupling matrix elements to "hallway states" extending to an excitation energy of 20 MeV. We

calculated separately the contributions from the isovector and isotensor components in order to study their interference.

### 2. Charge-symmetric–charge-dependent (CSCD) interaction

The CSCD interaction violates the equality of $V_{np}$ and $V_{nn}$ while maintaining $V_{nn}=V_{pp}$. Low energy scattering experiments give[19]

$$\frac{\Delta V_{CSCD}}{V_{CID}}=\frac{|\langle V_{np}\rangle|-|\langle V_{nn}\rangle|}{(|\langle V_{np}\rangle|+|\langle V_{nn}\rangle|)/2}$$

$$=0.0213\pm0.0052\ . \tag{3.13}$$

The quantities in brackets are spatial averages of potentials.

Approximately 65% of this CSCD comes from the mass difference between charged and neutral pions in the one-pion exchange potential (OPEP), and the remainder is accounted for by (1) this effect on the two-pion exchange potential (TPEP), (2) radiative corrections to the meson-nucleon coupling constants, and (3) meson-photon exchange effects.[20] These latter contributions to the CSCD interaction have different ranges from that of OPEP.

The fact that interactions with different ranges contribute to the CSCD interaction is important because the inclusion of two-nucleon correlation effects in $^{49}$Sc leads to a reduction of the CSCD interaction which might be expected to be larger for the components with shorter ranges. Following the procedures developed by Demos[21] and Rao[22] for finite nuclei, we therefore carried out a $G$-matrix calculation in $^{49}$Sc of the effect of correlations on the singlet matrix elements of the CSCD interaction arising both from the OPEP and TPEP. For both components we found a reduction factor due to correlations of approximately 20%.

For the CSCD interaction used in our calculations of the spreading width we used the OPEP form with its strength increased by about 1.5 to account for the observed departure from charge independence. We then applied a factor of 0.80 for the reduction arising from correlations. The resulting interaction has a strength of $V_0'=13.4$ MeV and a radial dependence given by

$$v_{CSCD}(1,2)=V_0'\tau_3(1)\tau_3(2)\frac{e^{-\mu' r}}{\mu' r}$$

$$\times[1-(\mu/\mu')^2 e^{(\mu'-\mu)r}]\ , \tag{3.14}$$

where $\mu'$ and $\mu$ refer to the charged and neutral mesons, respectively. The $s$-wave matrix elements of this interaction are negative, so that it is attractive for like nucleons and repulsive for unlike nucleons.

### 3. Charge asymmetric (CACD) interaction

The magnitude and form of a charge asymmetric component of the two-nucleon interaction remain unknown. Results from low-energy scattering experiments show that charge symmetry is more nearly exact for the short-range component than is charge independence.[19,23] After subtraction of the electromagnetic effects the scattering length and effective range for pp scattering are $a_{pp}=-17.2\pm3.0$ fm and $r_{pp}=2.84\pm0.03$ fm. The large uncertainty in $a_{pp}$ reflects its sensitivity to the short-range part of the interaction. The nn scattering length and effective range have been extracted from the reactions $\pi^-\mathrm{d}\rightarrow\mathrm{nn}\gamma$, nnH$\rightarrow$nnp, and $^3$H($^3$H,$^4$He)nn. Averaging the experimental result from these reactions gives $a_{nn}=-16.4\pm1.2$ fm and $r_{nn}=2.84$ fm. On the other hand, the $^1S_0$ effective range parameters for neutron-proton scattering are $a_{np}=-23.715\pm0.015$ fm and $r_{np}=2.73\pm0.03$ fm.

The evidence for a sizable CACD component of the short-range two-nucleon interaction is the Nolen-Schiffer anomaly[2] in the Coulomb energy shifts between corresponding levels of mirror nuclei. A particular case is the Coulomb energy difference in $^{41}$Ca-$^{41}$Sc, which has been analyzed in detail by Negele.[24] Concluding that none of the known Coulomb effects could account for the anomaly in these nuclei, Negele proposed the existence of a small charge-asymmetric (CACD) interaction. As a result several investigations[25,26] have been carried out using phenomenological CACD (usually called CSB) interactions. Sato[26] has claimed success in accounting for the anomaly in the ground states of single-particle and single-hole nuclei with a particular CACD interaction which is consistent with the difference in the nn and pp scattering lengths. More recently Coon and Scadron[27] have completed a series of calculations of charge dependent interactions in nuclei[28] and have concluded that the CACD interaction can be accounted for by a sum of terms coming from two pion exchange,[27] $\rho^0$-$\omega$ mixing,[28] $\pi^0$-$\eta$ and $\pi$-$\eta^0$ mixing,[29] and simultaneous exchange of a $\gamma$ and a $\pi^0$.[30]

Shifts produced by short-range charge dependent components of the NN interaction are overwhelmed by the very large Coulomb shifts. As noted earlier, however, the spreading widths of the IAS are likely to be much more sensitive to charge-dependent components which have a short range. We therefore included a calculation of the contribution of a CACD interaction to the spreading width of the analog of $^{49}$Ca. In view of the complexity of the CACD interaction implied by the analysis of Coon and Scadron,[27] we decided to use the phenomenological CACD interaction determined by Sato.[26] For this purpose we used only the isovector component of the Sato interaction, since this is the only part of his interaction which actually breaks charge symmetry. This is also the only part of his interaction which actually contributes to the Nolen-Schiffer anomaly in the mirror nuclei, and therefore the only part which was determined by his studies on the anomalies in mirror nuclei. The CACD interaction we use is therefore

$$V_{CACD}(1,2)=-V_0\tfrac{1}{2}(\tau_3(1)+\tau_3(2))$$

$$\times[1.14+0.31\sigma(1)\cdot\sigma(2)]\frac{e^{-\mu r}}{\mu r}\ , \tag{3.15}$$

where Sato determined the strength to be $V_0=-0.478$ MeV. This is approximately 1% of the charge independent force, and more than a factor of 20 smaller than the

CSCD interaction. However, the CSCD interaction changes sign at 2.9 fm and its matrix elements are reduced by a cancellation between values for small and large radii, whereas the CACD interaction has the monotonic radial dependence of the Yukawa potential. The effective strength of the CSCD is only about 2% of the charge independent interaction, and it is therefore only about twice the strength of the CACD.

## IV. MICROSCOPIC CALCULATION

### A. Fine structure states

The $^{49}$Sc IAS corresponding to the ground state of $^{49}$Ca lies at an excitation energy of 11.6 MeV. To calculate the spreading width we considered all configurations up to 20 MeV, taking the single particle and hole energies from Table III. These are from Jaffrin and Ripka[31] with corrections based on more recent experimental work.[32–34] The spin assignment[35] of $1f_{5/2}$ to the 4.078 MeV state in $^{49}$Ca was modified[34] to $2p_{3/2}$. The effect on the s.p. energy of the $1f_{5/2}$ state is negligible because of the very small spectroscopic factor for this state. Significant change in the $2p_{1/2}$ energy was found by Struve *et al.*,[33] who changed the assignment of the 4.49 MeV state in $^{49}$Sc from $2p_{3/2}$ (Refs. 32 and 36) to $2p_{1/2}$. Since the spectroscopic factor is $S=0.7$, this changes the $2p_{1/2}$ significantly. This is our only modification of the Jaffrin and Ripka level scheme.

The orbits which must be considered in constructing FS configurations include $1d_{5/2}$, $1d_{3/2}$, $2s_{1/2}$, $1f_{7/2}$, $2p_{3/2}$, $1f_{5/2}$, $2p_{1/2}$, and $1g_{9/2}$. The total number of FS states with $T=\frac{7}{2}$ belonging to these configurations is of the order of 16000. Averaging the distribution of these $T_<$ states with a Lorentzian of width 2.0 MeV gives the average level density seen in Fig. 8. At the IAS at 11.6 MeV the average density is 0.170 keV$^{-1}$. This is in astonishingly good agreement with the value of 0.167 keV$^{-1}$ obtained from the average spacing of the resonances listed in Table I.

Many of these states cannot be coupled directly to the IAS. The number of states with $T=\frac{7}{2}$ which can be coupled directly to this IAS, the so-called hallway states, is only about 800. These hallway states are then coupled to more complicated states. We can obtain information on the mixing of hallway states with more complicated FS states by comparing the observed level density with the cumulative level density from 2p-1h, 3p-2h, 4p-3h, etc., configurations. The density of these p-h states is given by a formula of Williams[37] with parameters by Gilbert and Cameron.[38] The results given in Table IV indicate that the observed density of 0.167 keV$^{-1}$ requires complete mixing of hallway states with all configurations through 4p-3h. Thus the high resolution data on the IAS look deep into the compound nucleus, although the IAS doorway is a rather simple excitation.

### B. Reduction to hallway states

The mixing between hallway states and more complex configurations increases the number of states per unit energy interval which can be coupled to the IAS. However, the rms value for the coupling matrix elements to the resulting FS is reduced in the same proportion. Therefore the mixing of hallway states with more complicated configurations is not expected to change the IAS spreading width significantly, but this mixing greatly increases the task of calculating the spreading width.

We can reduce the scale of the calculation enormously by expressing $\Gamma^{\downarrow}$ entirely in terms of coupling matrix elements to hallway states only. This is easily done by using operator identities of Kerman and DeToledo Piza.[10]

$$\Gamma^{\downarrow}=2\sum_h \frac{(\Gamma_h^{\downarrow}/2+I)\,|\langle A\,|\,V_e\,|\,h\rangle|^2}{(E-E_h)^2+(\Gamma_h^{\downarrow}/2+I)^2}\,. \tag{4.1}$$

The quantities $\Gamma_h^{\downarrow}$ in this equation are the spreading widths of the hallway states, $\Gamma_h^{\downarrow}=2\pi\langle M_{hf}^2/D_f\rangle$, given by the Lorentz-weighted average of the squared matrix elements coupling each hallway state to more complex FS states. We shall evaluate $\Gamma^{\downarrow}$ by using an average value $\langle\Gamma_h^{\downarrow}\rangle$ for the hallway widths. The range of reasonable values is 1–3 MeV.

### C. Evaluation of the spreading matrix elements

Even though we have considerably reduced the scale of the calculation, the evaluation of the matrix elements between the IAS and the hallway states is a formidable task because we must use eigenstates of isospin. Figure 4 illustrates the fact that the IAS is a superposition of 1p-0h and 2p-1h states. Figure 4 also shows that a 2p-1h hallway state may also have 4p-3h components in order to be an eigenstate of isospin. The $m$p-$n$h classification of ex-

TABLE III. Particle energies relative to the ground state of $^{49}$Sc.

| Orbits | $\epsilon$ (p) (MeV) | $\epsilon$ (n) (MeV) |
|---|---|---|
| $1g_{9/2}$ | 8.50 | −1.12 |
| $1f_{5/2}$ | 5.95 | −1.18 |
| $2p_{1/2}$ | 5.68 | −3.12 |
| $2p_{3/2}$ | 4.42 | −5.14 |
| $1f_{7/2}$ | 0 | −9.94 |
| $2s_{1/2}$ | −5.64 | −13.63 |
| $1d_{3/2}$ | −6.01 | −13.64 |
| $1d_{5/2}$ | −9.79 | −16.57 |

TABLE IV. Density of particle-hole states at 11.6 MeV in $^{49}$Sc.

| Complexity | Number of states per MeV | Cumulative level density per keV |
|---|---|---|
| 2p-1h | 4 | 0.004 |
| 3p-2h | 42 | 0.045 |
| 4p-3h | 70 | 0.111 |
| 5p-4h | 21 | 0.143 |

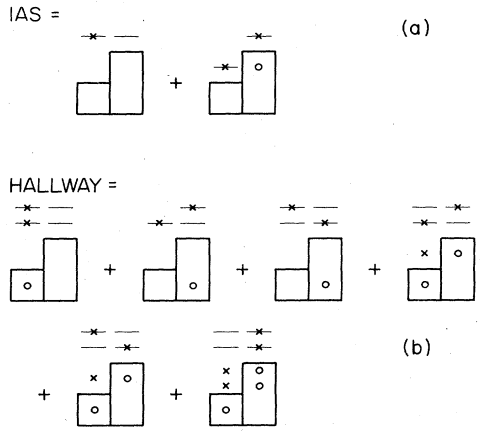


FIG. 4. The particle-hole components of the analog of $^{49}$Ca are illustrated in (a), with neutron orbits to the right and proton orbits to the left. Below this part (b) shows the components of one of the hallway states. The 3p-2h and 4p-3h components must be added to the 2p-1h component to make a state of isospin $T_< = \frac{7}{2}$.

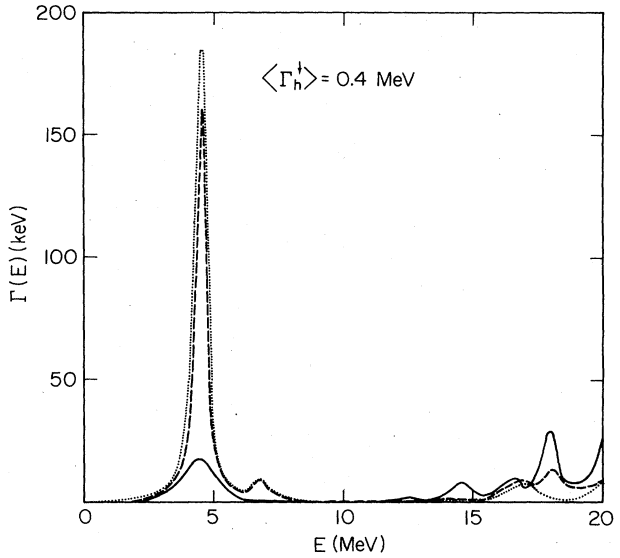


FIG. 5. Width functions $\Gamma^{\downarrow}(E)$ are shown for the isovector $\cdots$ and isotensor — — — components of the Coulomb interaction. The solid curve is $\Gamma^{\downarrow}(E)$ for the coherent sum of the two sets of matrix elements. A value of $\langle \Gamma_h^{\downarrow} \rangle = 0.4$ MeV is used to highlight the coherence.

cited states is useful here only for identifying the hallway *component* of a FS state.

In the shell model multiparticle matrix elements are usually evaluated by a standard method which separates out two-particle wave functions from totally antisymmetric multiparticle states by using order preserving permutations and coefficients of fractional parentage (cfp). The hallway states have from six to ten nucleons in the $1f_{7/2}$ shell. This presents us with a very open shell problem because 16 particles are required to close the $1f_{7/2}$ orbits in the isospin representation, in contrast with the 8 required in the proton-neutron representation. We were not able to employ standard techniques for reducing the multiparticle matrix elements because of the limited range of existing tables of cfp's. However, by constructing a complete set of hallway states characterized by the coupling of various subgroups of nucleons and by employing order preserving permutations, we found it possible to evaluate all of the necessary two-body matrix elements directly in terms of vector coupling coefficients.[39]

## V. DISCUSSION OF RESULTS

We have calculated $\Gamma_A^{\downarrow} = \Gamma^{\downarrow}$ (11.6 MeV) with the inclusion of the various charge-dependent components of the NN interaction which were discussed in Sec. III. Reasonable estimates for the average hallway spreading width lie in the range $\langle \Gamma_h \rangle = 1.5$–$3.0$ MeV. Table V gives the results of our calculations of the various contributions to $\Gamma_A^{\downarrow}$ for several values of $\langle \Gamma_h \rangle$ in this range.

First note that $\Gamma_A^{\downarrow}$ is in excellent agreement with the value of $\Gamma_A^{\downarrow} = 5.3 \pm 0.5$ keV obtained from the strength function analysis of the experimental data. Second, note that according to Table V the various charge-dependent interactions contribute *coherently* to $\Gamma_A^{\downarrow}$. Although the matrix elements of the CSCD interaction would only give rise to a spreading width of about 1 keV, and the first- and second-order Coulomb matrix elements would only give a spreading width of 3.5–3.9 keV, together these two sets of matrix elements generate a spreading width of 6.9–7.5 keV. Again, although the CACD interaction would give a spreading width of only 0.3 keV, when added coherently to the matrix elements of the CSCD interaction and the Coulomb interaction the CACD interaction reduces the spreading width by almost 1 keV. Comparing the fourth and fifth columns of Table V with the sixth column, we again see a strong coherence between the

TABLE V. Contributions to the spreading width of the analog of $^{49}$Ca.

| | Direct Coulomb | | | Individual contributions (keV) | | | | | |
|---|---|---|---|---|---|---|---|---|---|
| $\langle \Gamma_h^{\downarrow} \rangle$ (MeV) | isovector | isotensor | total | IVM | Coulomb + IVM | CSCD | Coulomb + IVM + CSCD | CACD | Total $\Gamma_A^{\downarrow}$ |
| 1.5 | 1.37 | 1.46 | 1.25 | 3.09 | 3.21 | 0.97 | 5.80 | 0.312 | 5.06 |
| 2.0 | 1.70 | 1.82 | 1.65 | 3.47 | 3.45 | 1.06 | 6.89 | 0.321 | 5.61 |
| 2.5 | 2.00 | 2.15 | 2.03 | 3.72 | 3.64 | 1.12 | 7.16 | 0.325 | 6.10 |
| 3.0 | 2.28 | 2.46 | 2.40 | 3.88 | 3.84 | 1.19 | 7.45 | 0.330 | 6.58 |

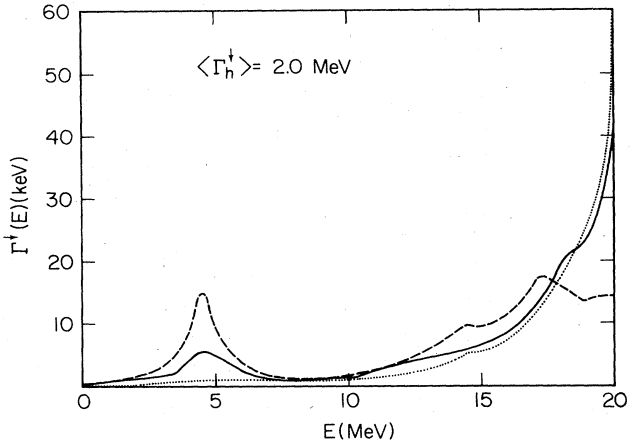


FIG. 6. Width function $\Gamma^{\downarrow}(E)$ for the direct Coulomb coupling $\cdots$ and for the second-order coupling through the IVM — — —. The solid curve of $\Gamma^{\downarrow}(E)$ for the coherent sum of these matrix elements shows destructive interference near the configuration states.

direct and the second-order Coulomb spreading. The total Coulomb spreading width is approximately that given by the IVM alone, but it would be wrong to conclude that the direct Coulomb matrix elements are negligible. The same coherence evidently exists between the isovector and isotensor components of the direct Coulomb matrix elements. The two contributions to the spreading width are comparable, but the coherent sum is close to that of the isovector component alone.

A plot of $\Gamma^{\downarrow}(E)$, given by Eq. (4.1), as a function of energy shows that the spreading matrix elements of the various charge-dependent interactions are actually coherent at all energies rather than at just the energy of the IAS. This is best seen by treating $\langle\Gamma_h^{\downarrow}\rangle$ as an arbitrary parameter and choosing a small value for it, say 0.4 MeV. For example, Fig. 5 shows that the isovector and isotensor components of the direct Coulomb coupling have very large matrix elements to the antianalog and other configuration states near 5 MeV, seen in the large peaks there. But

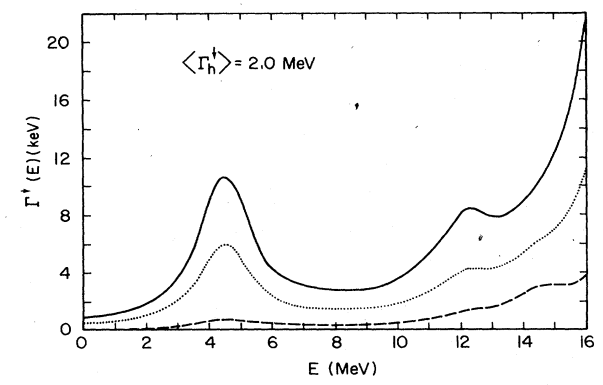


FIG. 7. Width functions $\Gamma^{\downarrow}(E)$ for the total Coulomb (direct plus IVM) coupling $\cdots$ and for the CSCD — — —. The solid curve is $\Gamma^{\downarrow}(E)$ for the coherent sum of these two sets of matrix elements.

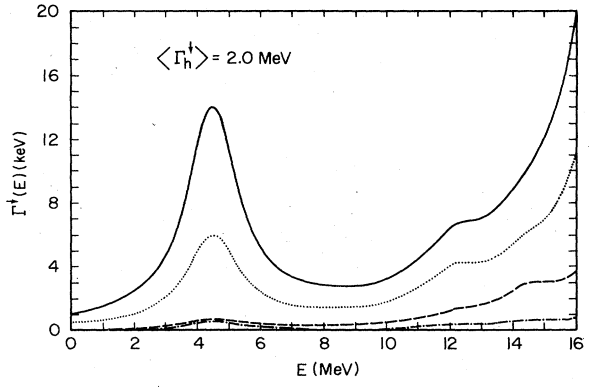


FIG. 8. Width functions $\Gamma^{\downarrow}(E)$ for the total Coulomb $\cdots$, the CSCD — — —, and the CACD —·—·— matrix elements. The solid curve shows $\Gamma^{\downarrow}(E)$ for the coherent sum of the three sets of matrix elements.

these two sets of matrix elements interfere destructively when added, resulting in a reduction of the direct Coulomb coupling to the configuration states by a factor of more than 70.

This reduction is easily understood. The separate isovector and isotensor Coulomb matrix elements between the IAS and the configuration states are dominated by the monopole component of the Coulomb interaction. Added coherently these two components give the isovector monopole interaction of Eq. (3.11), which does not couple to the configuration states in $^{49}$Sc. This leaves only the higher order multipoles to couple directly the analog to the configuration states.

Destructive interference also occurs between the direct Coulomb coupling to the antianalog and that going through the IVM. Figure 6 shows that the coupling through the IVM is reduced by a factor of 4. From Table V one finds that for $\langle\Gamma_h^{\downarrow}\rangle$=2.0 MeV the first- and second-order Coulomb coupling would give $\Gamma_A^{\downarrow}$=3.45 keV, to be compared to 3.47 keV for the IVM alone.

In Fig. 7 can be seen the constructive interference between the total Coulomb spreading and that contributed by the CSCD interaction which is reflected in Table V.

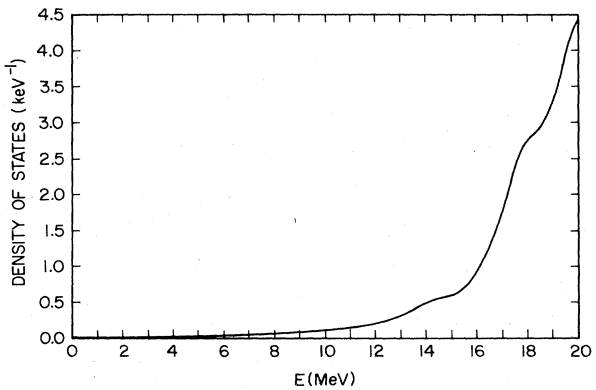


FIG. 9. Average level density of FS states obtained with a Lorentz averaging function with a width of 2.0 MeV.

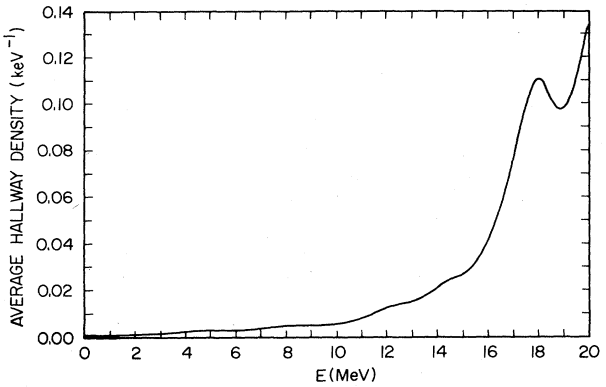


FIG. 10. Average level density of hallway states obtained with a Lorentz averaging function with a width of 2.0 MeV.

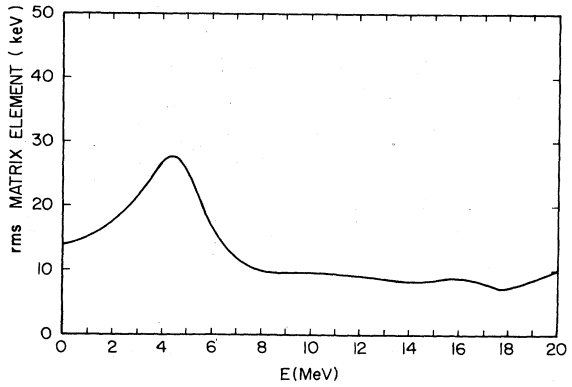


FIG. 11. Root-mean-square of matrix elements from IAS to hallway states.

Note that the matrix elements add coherently everywhere. Figure 8 shows how relatively important the Coulomb, the CSCD, and the CACD spreading widths are. This figure again shows the importance of coherence between the Coulomb matrix elements and those of the CSCD interaction. Comparison of Fig. 7 with Fig. 8 suggests that the energy dependence of $\Gamma^{\downarrow}(E)$ may be a reflection of the density of hallways. Figure 9 shows the average level density of FS states obtained with a Lorentz averaging function with a width of 2.0 MeV. In Fig. 10 we plot the density of hallway states, obtained by using the same Lorentz averaging function with a width of 2.0 MeV. From the ratio of $\Gamma^{\downarrow}(E)$ to this density of hallway states we can find the rms value of the spreading matrix elements to the hallway states located at various energies. This is shown in Fig. 11. Indeed, we see that the rms value of the coupling matrix elements is remarkably constant at about $9\pm1$ keV for hallway states in the entire energy range 8—20 MeV. In spite of the partial cancellation between the isovector and isotensor components of the Coulomb interaction, however, Fig. 10 shows that the matrix elements to the antianalog and the other configuration states are larger than those to other hallway states.

## VI. SUMMARY AND CONCLUSIONS

We have found that the contribution of short-range charge-dependent interactions to the spreading width of the analog of $^{49}$Ca is relatively much larger than the Coulomb displacement anomaly. This result confirms the general expectation that the violations of isospin selection rules on transition matrix elements are much more sensitive to contributions from short-range charge-dependent interactions than are level shifts. In $^{49}$Sc we have found that the CSCD interaction contributes approximately one-half of the observed spreading width of the $^{49}$Ca analog.

A CACD interaction, which is sufficient to account for the breaking of charge symmetry seen in the Coulomb anomaly in the mirror pair $^{41}$Sc-$^{41}$Ca, also contributes coherently to $\Gamma^{\downarrow}_A$. However, the resulting reduction of $\Gamma^{\downarrow}_A$ by about 1 keV is too small to establish the presence of a CACD interaction in light of the uncertainty in both the experimental and calculated values of $\Gamma^{\downarrow}_A$.

The most important conclusion to be drawn from this work is that the known CSCD interaction cannot be neglected in any calculation which seeks to account for the spreading widths of the IAS. In fact, although the microscopic calculations of these widths are formidable, they may well provide the best information on the importance of short-range charge-dependent interactions in nuclei.

## ACKNOWLEDGMENTS

With pleasure we acknowledge many helpful conversations with M. K. Banerjee. Support of the U. S. Department of Energy for this research is gratefully acknowledged. Support for the calculations was also provided by the Computer Science Center of the University of Maryland at College Park.

*Present address: Department of Physics and Astronomy, University of Pittsburgh, Pittsburgh, PA 15260.

[1]A. Z. Mekjian, Phys. Rev. Lett. **25**, 888 (1970).
[2]J. A. Nolan and J. P. Schiffer, Annu. Rev. Nucl. Sci. **19**, 471 (1969).
[3]S. Shlomo, Rep. Prog. Phys. **41**, 957 (1978).
[4]P. Wilhjelm *et al.*, Phys. Rev. **177**, 1553 (1968).
[5]J. B. McGrory, B. H. Wildenthal, and E. C. Halbert, Phys. Rev. C **2**, 186 (1970).
[6]D. M. Brink and J. P. Svenne, Nucl. Phys. **A154**, 449 (1970).
[7]*Nuclear Analog States,* edited by D. Robson and John D. Fox (Dowden, Hutchison, and Ross, Stroudsburg, 1976).

[8]W. M. MacDonald and A. Mekjian, Phys. Rev. **160**, 730 (1967).
[9]A. Z. Mekjian and W. M. MacDonald, Nucl. Phys. **A121**, 385 (1968).
[10]A. K. Kerman and A. F. R. De Toledo Piza, Ann. Phys. (N.Y.) **48**, 173 (1968).
[11]W. M. MacDonald, Ann. Phys. (N.Y.) **125**, 253 (1980).
[12]W. M. MacDonald, Phys. Rev. C **20**, 426 (1979).
[13]W. M. MacDonald, Phys. Rev. **100**, 51 (1955).
[14]A. Bohr, J. Damgaard, and B. R. Mottelson, reported in A. Bohr and B. R. Mottelson, *Nuclear Structure* (North-Holland, Amsterdam, 1967).
[15]For a recent discussion of the IVM, see N. Auerbach, Phys. Rep. **98**, 273 (1983).
[16]N. Auerbach, Nucl. Phys. **A182**, 247 (1972).
[17]W. M. MacDonald and N. Auerbach, Phys. Lett. **52B**, 425 (1975).
[18]G. E. Brown, L. Castillejo, and J. A. Evans, Nucl. Phys. **22**, 1 (1961); W. L. Wang and C. M. Shakin, Phys. Rev. C **5**, 1898 (1972); R. H. Lemmer and C. M. Shakin, Ann. Phys. (N.Y.) **27**, 13 (1964); R. W. Sharp and L. Zamick, Nucl. Phys. **A208**, 130 (1973).
[19]E. M. Henley, in *Isospin in Nuclear Physics,* edited by D. H. Wilkinson (North-Holland, Amsterdam, 1969).
[20]T. E. O. Ericson and G. A. Miller, Phys. Lett. **B132**, 32 (1983).
[21]J. R. Demos, doctoral dissertation, University of Maryland, 1970.
[22]S. Y. Rao, doctoral dissertation, University of Maryland, 1972.
[23]E. M. Henley and G. A. Miller, in *Mesons in Nuclei,* edited by M. Rho and D. H. Wilkinson (North-Holland, Amsterdam, 1979).
[24]J. Negele, Nucl. Phys. **A165**, 305 (1971).
[25]S. Shlomo, Phys. Lett. **42B**, 146 (1972); S. Shlomo and D. O. Riska, Nucl. Phys. **A254**, 281 (1975).
[26]H. Sato, Nucl. Phys. **A269**, 378 (1976).
[27]S. A. Coon and M. D. Scadron, Phys. Rev. C **26**, 562 (1982).
[28]P. C. McNamee, M. D. Scadron, and S. A. Coon, Nucl. Phys. **A249**, 483 (1975); S. A. Coon, M. D. Scadron, and P. C. McNamee, *ibid.* **A287**, 381 (1977).
[29]S. A. Scadron and S. A. Coon, Phys. Rev. C **26**, 562 (1982).
[30]D. O. Riska and Y. H. Chu, Nucl. Phys. **A235**, 499 (1974); P. U. Sauer and H. Walliser, J. Phys. G **3**, 1513 (1977).
[31]A. Jaffrin and G. Ripka, Nucl. Phys. **A119**, 529 (1968).
[32]E. Eichler and S. Raman, Phys. Rev. C **3**, 2268 (1971).
[33]H. Struve *et al.*, Phys. Rev. C **4**, 471 (1971).
[34]W. D. Metz, W. D. Callender, and C. K. Bokelman, Phys. Rev. C **12**, 827 (1975).
[35]E. Kashy *et al.*, Phys. Rev. **135**, B865 (1964); T. R. Canada, C. Ellegaard, and P. D. Barnes, Phys. Rev. C **4**, 471 (1971).
[36]J. R. Erskine, A. Marinov, and J. P. Schiffer, Phys. Rev. **142**, 633 (1966).
[37]F. C. Williams, Jr., Nucl. Phys. **A109**, 231 (1971).
[38]A. Gilbert and A. G. W. Cameron, Can. J. Phys. **43**, 1446 (1965).
[39]G.-K. Kim, doctoral dissertation, University of Maryland, 1983.